

RESEARCH REPORT

Girdin-mediated interactions between cadherin and the actin cytoskeleton are required for epithelial morphogenesis in *Drosophila*

Elise Houssin¹, Ulrich Tepass² and Patrick Laprise^{1,*}

ABSTRACT

E-cadherin-mediated cell-cell adhesion is fundamental for epithelial tissue morphogenesis, physiology and repair. E-cadherin is a core transmembrane constituent of the *zonula adherens* (ZA), a belt-like adherens junction located at the apicolateral border in epithelial cells. The anchorage of ZA components to cortical actin filaments strengthens cell-cell cohesion and allows for junction contractility, which shapes epithelial tissues during development. Here, we report that the cytoskeletal adaptor protein Girdin physically and functionally interacts with components of the cadherin-catenin complex during *Drosophila* embryogenesis. Fly Girdin is broadly expressed throughout embryonic development and enriched at the ZA in epithelial tissues. Girdin associates with the cytoskeleton and co-precipitates with the cadherin-catenin complex protein α -Catenin (α -Cat). *Girdin* mutations strongly enhance adhesion defects associated with reduced DE-cadherin (DE-Cad) expression. Moreover, the fraction of DE-Cad molecules associated with the cytoskeleton decreases in the absence of Girdin, thereby identifying Girdin as a positive regulator of adherens junction function. *Girdin* mutant embryos display isolated epithelial cell cysts and rupture of the ventral midline, consistent with defects in cell-cell cohesion. In addition, loss of Girdin impairs the collective migration of epithelial cells, resulting in dorsal closure defects. We propose that Girdin stabilizes epithelial cell adhesion and promotes morphogenesis by regulating the linkage of the cadherin-catenin complex to the cytoskeleton.

KEY WORDS: Girdin, GIV, Epithelial tissues, Epithelial morphogenesis, Cell-cell adhesion, E-cadherin, Armadillo, *Drosophila melanogaster*

INTRODUCTION

Cell motility plays a fundamental role during animal development and is essential for tissue homeostasis (Friedl and Gilmour, 2009). The cytoskeletal adaptor protein Girdin emerged recently as an important positive regulator of cell migration in various mammalian cell types (Enomoto et al., 2005; Ghosh et al., 2008; Jiang et al., 2008; Kitamura et al., 2008; Wang et al., 2011). Girdin directly interacts with actin microfilaments through its C-terminus (Enomoto et al., 2005, 2006; Jiang et al., 2008). Depletion of Girdin impairs actin organization at the leading edge of migrating

cells and results in directional cell locomotion defects (Enomoto et al., 2005; Ohara et al., 2012). It has been shown recently that Girdin binds to the polarity protein Par-3 (Ohara et al., 2012). Cells depleted for either Girdin or Par-3, or expressing a mutant Par-3 protein unable to interact with Girdin, failed to polarize in the direction of migration (Enomoto et al., 2005; Ohara et al., 2012). In addition to playing a broad role in cell polarity, Par-3 and its *Drosophila* ortholog Bazooka (Baz) act as crucial regulators of *zonula adherens* (ZA) assembly, positioning and stability (Harris and Peifer, 2004; McGill et al., 2009; Morais-de-Sá et al., 2010; Ooshio et al., 2007; Xue et al., 2013). The ZA is a belt-like adherens junction maintaining the cohesion of epithelial tissues (Harris and Tepass, 2010). The transmembrane protein E-cadherin is a core component of the ZA that indirectly interacts with actin microfilaments through cytoplasmic adaptor proteins, including β -Catenin [Armadillo (Arm) in flies] and α -Catenin (α -Cat) (Desai et al., 2013; Harris and Tepass, 2010). The association of Par-3 with Girdin raises the possibility that the latter plays a role in cell-cell adhesion and epithelial tissue morphogenesis. A role for Girdin in epithelial morphogenesis is supported by the fact that depletion of Girdin in MCF10A mammary epithelial cells interferes with the formation of acini with a single lumen (Ohara et al., 2012). However, epithelial tissues do not show any gross defects in *Girdin* knockout mice (Asai et al., 2012; Enomoto et al., 2009). This lack of prominent abnormalities could result from functional redundancy with the mammalian Girdin paralogs Daple and Gipie (Enomoto et al., 2006; Matsushita et al., 2011).

Drosophila melanogaster has a single Girdin ortholog that was recently implicated, using knockdown approaches, in actin organization and regulation of cell size in imaginal disks (Puseenam et al., 2009). Here, we present a mutational analysis of *Drosophila Girdin* (*Girdin*) and provide evidence that Girdin interacts with the cadherin-catenin complex at adherens junctions and plays an important role in epithelial morphogenesis.

RESULTS AND DISCUSSION

Girdin is enriched at the ZA in epithelial tissues

To analyze the function of Girdin in *Drosophila* embryonic development, we generated *Girdin* null mutations and Girdin-specific antibodies. Mutant alleles were created by imprecise excision of the P element *KG07727* (Bellen et al., 2004). We recovered several lethal alleles, including *Girdin*¹ and *Girdin*², which failed to complement an independent line carrying a PiggyBac transposon within the *Girdin* coding region [*Girdin*^{c06007}; supplementary material Fig. S1A; see Bellen et al. (2011); Thibault et al. (2004)]. Anti-Girdin antibodies revealed that Girdin is maternally provided and expressed throughout embryogenesis (Fig. 1A), as previously reported (Puseenam et al., 2009). In most embryonic stages, Girdin migrated as a triplet (Fig. 1A), which was not detected in

¹Department of Molecular Biology, Medical Biochemistry and Pathology/Cancer Research Center, Laval University, and CRCHU-oncology axis, Québec, Québec, Canada G1R 3S3. ²Department of Cell and Systems Biology, University of Toronto, Toronto, Ontario, Canada M5S 3G5.

*Author for correspondence (Patrick.Laprise@crchudequebec.ulaval.ca)

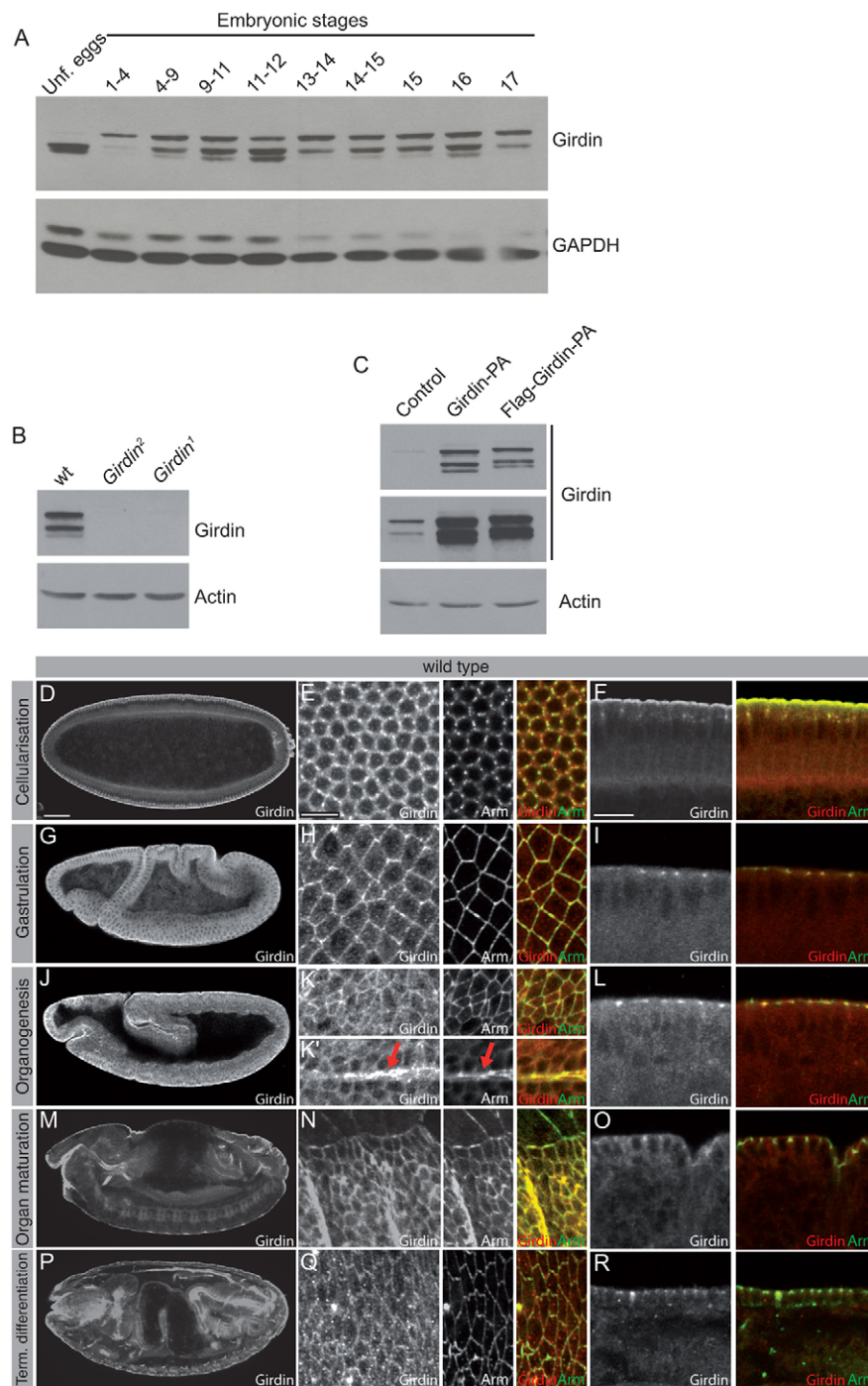


Fig. 1. Girdin is widely expressed in embryonic tissues and is concentrated at the ZA in epithelial cells. (A) Immunoblot showing the developmental expression profile of Girdin, which is also expressed in unfertilized eggs (Unf. eggs). (B) Western blot showing the complete loss of Girdin expression in *Girdin*¹ and *Girdin*² M/Z mutant embryos compared with wild-type (wt) embryos. Actin was used as loading control. (C) Stage 9-12 control (*daGAL4*; driver line), Girdin-PA-overexpressing (*Girdin*-PA; *daGAL4/UAS-Girdin*-PA) and Flag-tagged Girdin-PA (Flag-Girdin-PA)-expressing embryos were homogenized and processed for western blotting using anti-Girdin antibodies. Two expositions of the same blot are shown for Girdin. Actin was used as loading control. (D-F) Immunostaining of a cellularizing embryo with anti-Girdin and anti-Arm antibodies (red and green signal in merged pictures, respectively). Panels show a whole-embryo view of Girdin staining (D), a surface view of a portion of the blastoderm (E) or a lateral view of forming cells (F). (G-I) Immunostaining of Girdin and Arm in a gastrulating embryo: whole-embryo view (G, Girdin staining), surface view of the ectoderm (H) and lateral view of the ectoderm (I). (J) Panel depicts a stage-11 embryo immunostained for Girdin. (K) Surface view of a portion of the ventral ectoderm of a stage-11 embryo co-stained for Girdin and Arm. K' shows a deeper confocal section to highlight the ventral midline (red arrows). (L) Lateral view of the ectoderm of a stage-11 embryo showing the distribution of Girdin and Arm. (M-O) Immunostaining of a stage-14 embryo using anti-Girdin and anti-Arm antibodies (whole-embryo view of Girdin staining; M), surface view of the lateral epidermis (N), lateral view of epidermal cells (O). (P-R) Girdin and Arm distribution during terminal differentiation of embryonic tissues. Panels show a whole-embryo view (P), a surface view of the epidermis (Q) or a lateral view of epidermal cells (R). Scale bars: 50 μ m in D, also for G, J, M, P; 10 μ m in E, also for H, K, N, Q; 10 μ m in F, also for I, L, O, R.

Girdin mutant embryos (Fig. 1B). Thus, these three bands are bona fide products of the *Girdin* gene. Puseenam et al. reported two isoforms of Girdin in immunoblots, using a different anti-Girdin antibody, and assigned them to the two predicted isoforms Girdin-PA and Girdin-PB, expected to arise from alternative splicing (Puseenam et al., 2009). By contrast, we found that exogenous Girdin-PA, which is encoded by a cDNA corresponding to the longest isoform predicted (www.flybase.org; supplementary material Fig. S1A), showed an identical migration profile to endogenous Girdin (Fig. 1C). This suggests that Girdin is subject to post-translational modification, and that fly embryos mainly express the Girdin-PA isoform.

We investigated Girdin localization in developing embryos using our specific anti-Girdin antibody (supplementary material

Fig. S1B,C). Girdin protein is broadly distributed in embryos of all stages and showed a faint cytoplasmic distribution in most, if not all, cells. In addition, Girdin was enriched at the ZA in epithelial cells (Fig. 1D-R). Specifically, Girdin was enriched in pole cells and at the apex of forming epithelial cells at the end of cellularization (Fig. 1D). Girdin also marked spot adherens junction, as shown by its co-localization with Arm (Fig. 1E,F). During and after gastrulation, Girdin was concentrated at the ZA in ectodermal cells (Fig. 1G-I). Additionally, Girdin was expressed in the mesoderm and endoderm, where it showed a diffuse cytoplasmic distribution (Fig. 1G). During organogenesis, Girdin remained enriched at the ZA (Fig. 1J-L) and showed a strong accumulation together with Arm at the ventral midline (Fig. 1K', arrow). Girdin maintained its

ZA association in epithelial cells derived from the ectoderm until the end of embryogenesis (Fig. 1M-R). Moreover, Girdin was present in the midgut and the central nervous system (Fig. 1M,P). Our analysis revealed that Girdin is widely expressed in embryonic tissues and co-localizes with the cadherin-catenin complex in epithelia.

Girdin is required for proper epithelial sheet migration

To explore Girdin function, we used *Girdin*¹, *Girdin*² and *Girdin*^{c06007} mutant alleles. Similar to what has been reported for Girdin knocked-down flies (Puseenam et al., 2009), animals homozygous or trans-heterozygous for any allelic combinations died at pupal or pharate adult stages. Of note, the lethality is fully suppressed by ubiquitous expression of exogenous Girdin-PA, and the rescued adult flies were fertile. This illustrates that the observed phenotype specifically results from *Girdin* mutations, and that the additional predicted Girdin isoforms (www.flybase.org) are dispensable for the *Drosophila* life cycle. To investigate the phenotype associated with the complete loss of Girdin, we abolished the maternal contribution by generating *Girdin* germline clone females for all three alleles (Chou and Perrimon, 1996). Examination of the cuticle secreted by *Girdin* maternal and zygotic (M/Z) mutant embryos revealed several defects in epithelial tissue morphogenesis and integrity (Fig. 2A,B). *Girdin* mutant embryos showed impairment of head morphogenesis and loss of anterior structures such as mouth hooks (Fig. 2B). Embryos were also strewn with ectopic granules of cuticle (Fig. 2B,D, arrowheads; the origin of these grains of cuticle will be discussed in following sections). These defects were the same for all three alleles.

Immunostaining of the transmembrane protein Crumbs (Crb) revealed dorsal closure defects in *Girdin* mutant embryos (Fig. 2E,F, arrow). Crb staining also uncovered the presence of ectopic cell cysts and fragmentation of the dorsal trunk of the tracheal tree (Fig. 2F, red and yellow arrowheads, respectively). Dorsal closure failure in *Girdin* mutant embryos suggests that Girdin is essential for proper collective cell migration, which drives dorsal closure (Harden, 2002). Accordingly, some cells were dragging behind the leading edge of the lateral epidermis, which adopted an exaggerated wavy appearance at the onset of dorsal closure in *Girdin* M/Z embryos (compare Fig. 2G and H, arrows). Migrating cells of the lateral epidermis are polarized in the direction of migration in wild-type embryos, as their length along the dorso-ventral (D-V) axis is greater than their width (Fig. 2G, arrowhead). This polarization was delayed in *Girdin* mutant embryos in which most cells located behind the leading edge adopted a more symmetric shape at early stages of dorsal closure (Fig. 2H, arrowhead). These defects suggest that Girdin is important for the assembly of the supra-cellular F-actin cable that forms at the dorsal end of leading-edge cells [Fig. 2I, arrow; see Harden (2002); Kiehart et al. (2000)], as the contractile forces generated by this cable align leading-edge cells (Solon et al., 2009), contribute to the D-V elongation of epidermal cells and act as a purse string contributing to dorsal closure (Harden, 2002; Kiehart et al., 2000; Young et al., 1993). In support of this hypothesis, phalloidin staining and actin immunolabeling both revealed impaired actin accumulation in leading-edge cells in *Girdin* mutant embryos (Fig. 2I-L, arrow). This is consistent with previous findings showing that Girdin knockdown decreased the amount of F-actin in the wing disk (Puseenam et al., 2009). Loss of Girdin also caused a reduction in actin levels at the periphery of amniosera cells (Fig. 2I-L, arrowhead). This might contribute to epidermal migration defects in *Girdin* mutant embryos, as pulsed actomyosin-dependent contractions of amniosera cells contribute to dorsal closure (David et al., 2010; Franke et al., 2005; Kiehart et al., 2000; Solon et al., 2009). Together,

these results demonstrate that Girdin is essential for epithelial tissue morphogenesis, and that this protein shares an evolutionarily conserved function with mammalian Girdin in coordinating cell migration and in organizing the actin cytoskeleton (Weng et al., 2010).

Girdin supports epithelial cell cohesion and tissue integrity

Further analysis of the *Girdin* mutant phenotype revealed that cells at the ventral midline separated from each other in some *Girdin* M/Z mutants, thereby resulting in the opening of the ectoderm on the ventral side of embryos (Fig. 3A,C, arrowheads). In addition, some

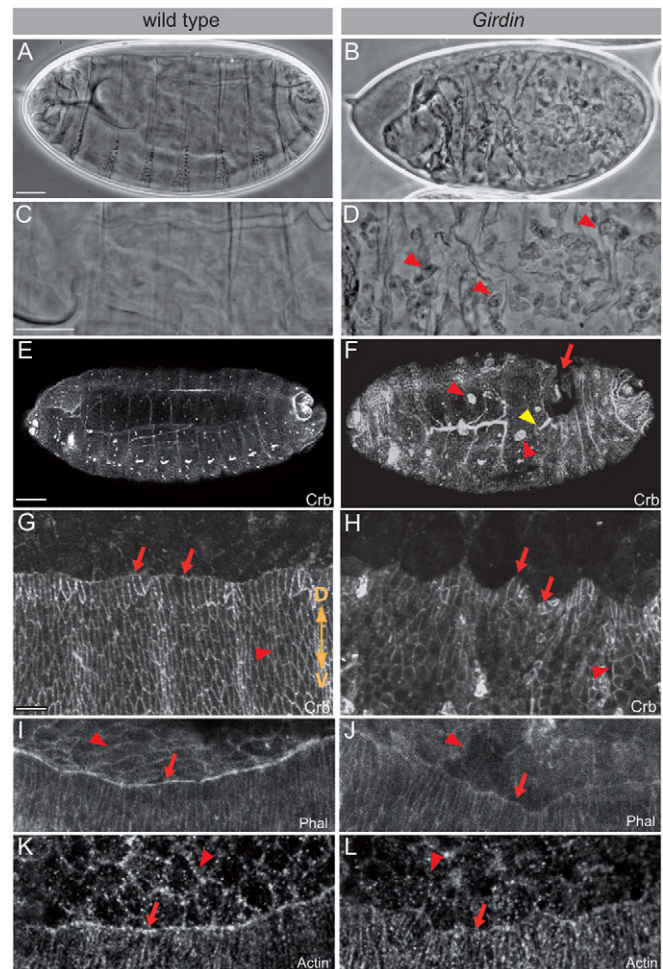


Fig. 2. Loss of Girdin impairs epithelial tissue integrity and dorsal closure. (A-D) Cuticle secreted by a wild-type embryo (A,C) or a *Girdin* M/Z mutant embryo (B,D). C and D are higher-magnification images of A and B, respectively. Anterior is to the left and dorsal is up. (E,F) Whole-embryo view of stage-16 wild-type embryo (E) or *Girdin* M/Z mutant embryo (F) immunostained for Crb. Arrow points to a persistent dorsal hole. The yellow arrowhead shows fragmentation of the dorsal trunk of the tracheal tree, whereas red arrowheads indicate ectopic cell cysts. (G,H) Wild-type or *Girdin* M/Z mutant embryos were immunostained using anti-Crb antibodies. Panels show a surface view of the lateral epidermis of late stage-13 wild-type (G) or *Girdin* M/Z mutant (H) embryos. Dorsal (denoted by D) side of embryos is up, ventral (labeled V) is down. (I,J) Stage-14 wild-type or *Girdin* M/Z mutant embryos were incubated with fluorescent phalloidin to stain F-actin. (K,L) Immunostaining of Actin on stage-14 wild-type (K) or *Girdin* M/Z mutant (L) embryos. (I-L) Arrows point to the cell row at the leading edge of the migrating epidermis, arrowheads indicate amniosera cell boundaries. Scale bars: 50 μ m in A, also for B; 10 μ m in C, also for D; 50 μ m in E, also for F; 10 μ m in G, also for H-L.

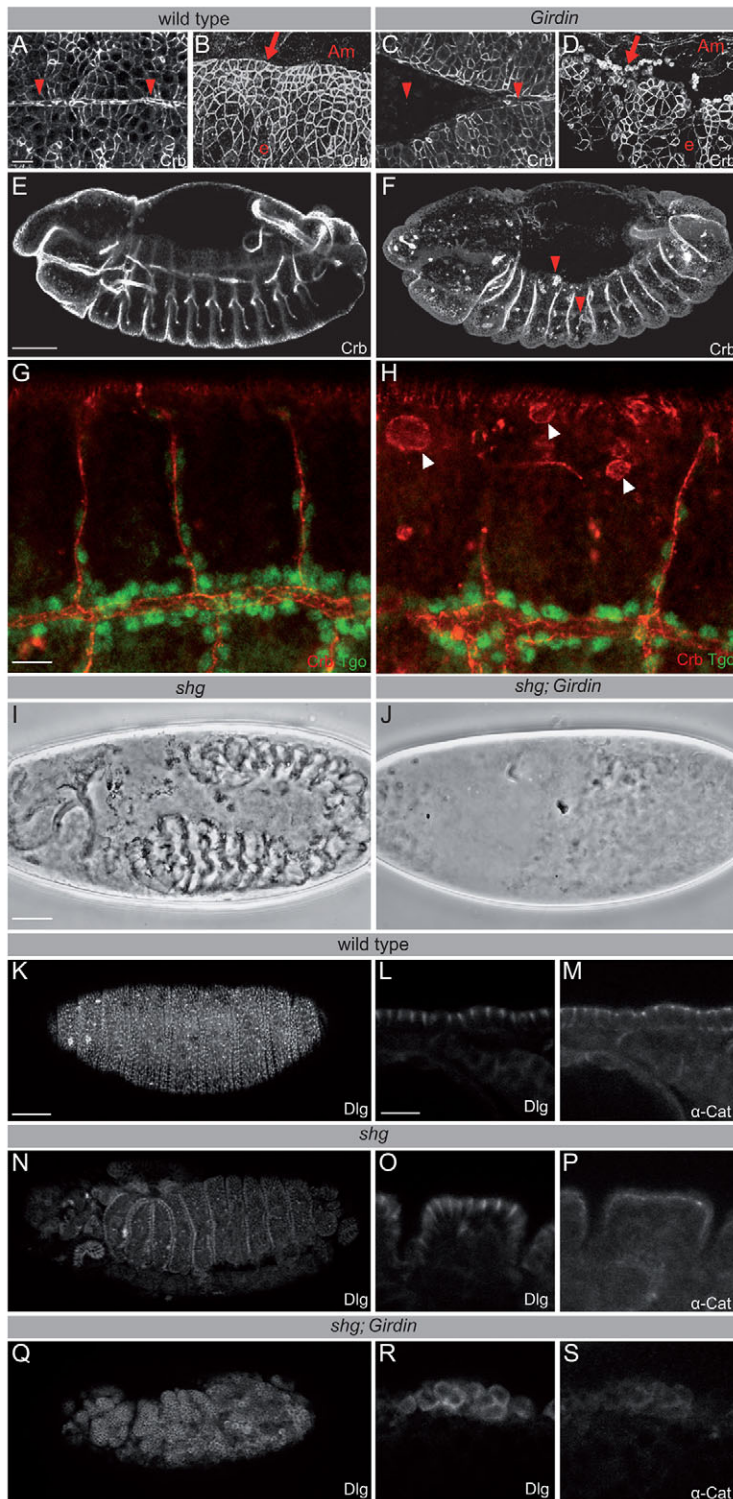


Fig. 3. Loss of Girdin causes epithelial cohesion defects.

(A-D) Immunostaining of Crb in wild-type (A,B) or *Girdin* M/Z mutant (C,D) embryos. A and C show the ventral midline (arrowheads) crossing the center of panels horizontally (anterior of the embryo is on the left). B and D show a surface view of the ectoderm (e) and of the amnioserosa (Am). Depicted embryos were at stage 11.

(E,F) Immunostaining of Crb in stage-13 wild-type (E) or *Girdin* M/Z mutant (F) embryos. Arrowheads point to epithelial cell cysts found below the epidermis. (G,H) Co-staining of Crb (red) and Tgo (green) in stage-15 wild-type (G) or *Girdin* M/Z mutant (H) embryos. Arrowheads show epithelial cell cysts, which are negative for the tracheal marker Tgo. (I,J) Cuticle secreted by a *shg* zygotic (Z) mutant embryo (I) or a *shg* (Z); *Girdin* M/Z mutant embryo (J). Anterior is left and dorsal is up. (K-S) Staining of Dlg and α -Cat in wild-type embryos (K-M), or *shg* (Z) (N-P) or *shg* (Z); *Girdin* M/Z (Q-S) mutant embryos. K,N and Q depict a whole-embryo view, whereas panels L,M,O,P,R,S show a lateral view of a portion of the epidermis. Scale bars: 10 μ m in A, also for B-D; 50 μ m in E, also for F; 10 μ m in G, also for H; 50 μ m in I, also for J; 50 μ m in K, also for N,Q; 10 μ m in L, also for M,O,P,R,S.

ectodermal cells in contact with the amnioserosa detached from the rest of the tissue in the absence of Girdin (compare Fig. 3B and D, arrow). The epithelial origin of these cells is confirmed by the expression of Crb, which is confined to epithelial tissues at this stage of embryogenesis (Tepass et al., 1990). Finally, *Girdin* null embryos display ectopic Crb expressing cell cysts (Fig. 2F and Fig. 3E,F, arrowheads). These cysts are located just below the epidermis from stage 10 onward, and are abundant in stage 13 and later stages of embryogenesis (Fig. 3F,H, arrowheads). Cyst cells

were negative for the tracheal marker Tango (Tgo; Fig. 3G,H, arrowheads), indicating that they do not originate from collapsed tracheal tubes, but probably from fragmentation of the overlying epidermis. This conclusion is consistent with the presence of sub-epidermal vesicles of cuticle characteristic of epidermal cells in embryos devoid of Girdin (Fig. 2B,D). Collectively, these observations highlight epithelial cohesion defects in *Girdin* mutant embryos, and thus suggest that Girdin contributes to cell-cell adhesion in epithelial tissues.

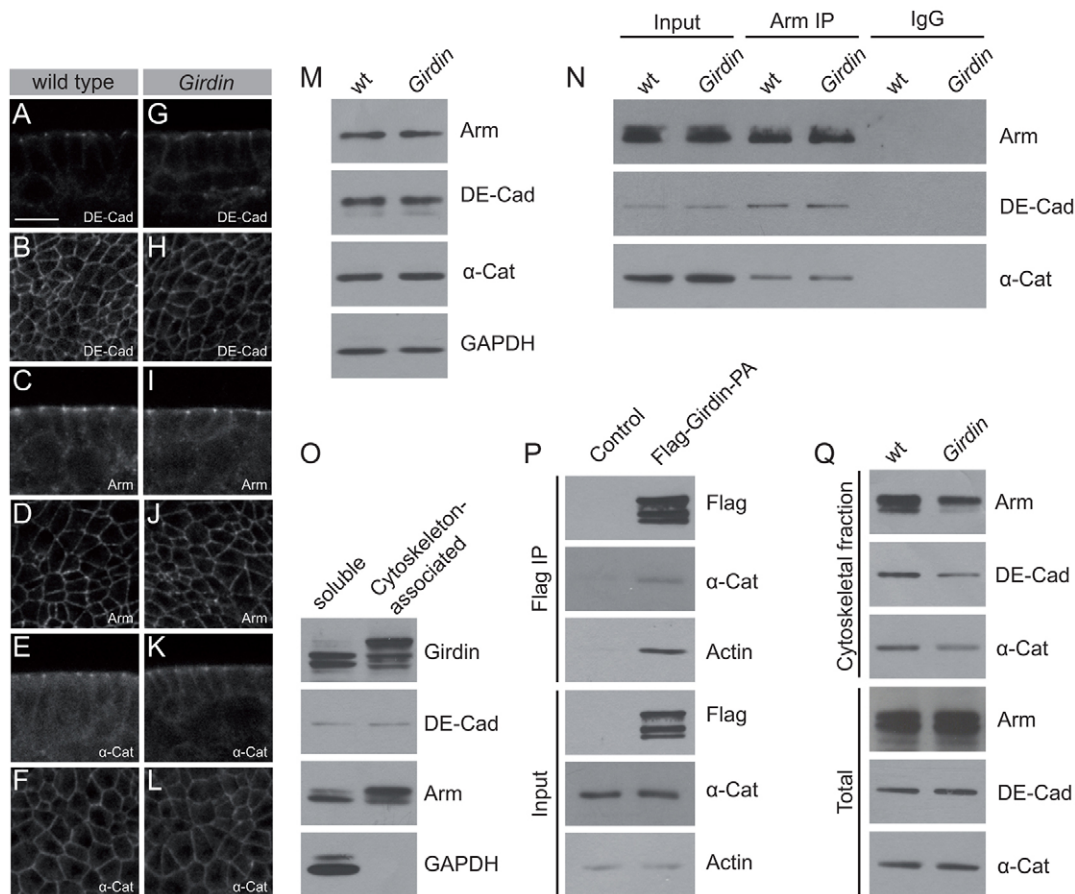


Fig. 4. Girdin is required for the association of Arm, DE-Cad and α -Cat with the cytoskeleton. (A-L) Wild-type embryos (A-F) or *Girdin* M/Z mutant embryos (G-L) were immunostained using antibodies directed against DE-Cad, Arm or α -Cat. Panels depict lateral view (A,C,E,G,I,K) or surface view (B,D,F,H,J,L) of the ectoderm of stage-11 embryos. (M) Western blotting showing the relative expression level of DE-Cad, Arm and α -Cat in *Girdin* M/Z mutant embryos compared with their wild-type counterparts. GAPDH was used as loading control. (N) Endogenous Arm was immunoprecipitated with a wild-type embryo lysate (Arm IP). Mouse IgG (IgG) purified from a non-immune serum was used as negative control. Western blot using anti-Arm, anti-DE-Cad and anti- α -Cat antibodies revealed that the immunoprecipitation was effective and that DE-Cad and α -Cat co-precipitated with Arm. A portion of each homogenate was kept to monitor expression of Arm, DE-Cad and α -Cat (input). (O) Soluble and cytoskeleton-associated proteins were fractionated from wild-type embryos. Western blots show the distribution of Girdin, DE-Cad, Arm and GAPDH in these fractions. (P) Flag-tagged Girdin was immunoprecipitated with anti-Flag antibodies (Flag IP). A Flag immunoprecipitation was performed on control embryos as negative control. Western blotting revealed the presence of Girdin, Actin and α -Cat in the immunocomplex. A portion of each homogenate was used to monitor expression of Flag-Girdin, Actin and α -Cat (input). (Q) Cytoskeleton-associated proteins from wild-type and *Girdin* M/Z mutant embryos were processed for western blotting, using antibodies directed against Arm, DE-Cad and α -Cat. The total expression level of these proteins is also shown.

Despite prominent cohesion defects, most epidermal cells remained attached to each other in *Girdin* mutant embryos (Fig. 2E-L and Fig. 3C,D). Similarly, large patches of coherent epidermal cells and cuticle layers remained in zygotic (*Z*) *shotgun* (*shg*; encoding DE-Cad) mutant embryos [Fig. 3L,N; see Tepass et al. (1996); Uemura et al. (1996)]. By contrast, loss of Girdin in a *shg* (*Z*) mutant background resulted in an almost complete absence of cuticle, with the residual cuticle forming isolated morsels (Fig. 3J), as observed in *shg* M/Z or *arm* M/Z embryos (Muller and Wieschaus, 1996; Tepass et al., 1996). This phenotype reflects collapse of epithelial tissues in these embryos (Fig. 3Q). Moreover, staining of the lateral protein Dlg revealed that cells adopted a rounded morphology and loosely adhered to each other in *shg* (*Z*) *Girdin* (M/Z) mutant embryos (compare Fig. 3R with L and O). Adhesion defects in these embryos are further revealed by a near-complete loss of α -Cat at cell-cell contacts (Fig. 3M,S). The striking enhancement of the *shg* (*Z*) phenotype associated with the loss of Girdin suggests that Girdin contributes to DE-Cad-mediated cell-cell adhesion. Together, these results indicate that Girdin strengthens or stabilizes adherens junctions in support of epithelial tissue integrity.

Girdin regulates the link between the cadherin-catenin complex and the cytoskeleton

To better define the role of Girdin in epithelial tissue cohesion, we investigated crucial features of cadherin-mediated cell-cell adhesion in *Girdin* mutant embryos. First, ZA formation and maintenance require the balance between E-cadherin delivery, endocytosis and recycling (Kowalczyk and Nanes, 2012). Mammalian Girdin controls dynamin 2 activity, thereby favoring endocytosis of selected cargoes such as E-cadherin, which adopted a patchy distribution in Girdin-deficient MDCK cells (Simpson et al., 2005; Weng et al., 2014). However, Girdin knockdown does not alter E-cadherin distribution in MCF10A cells (Ohara et al., 2012). Similarly, the localization and expression levels of DE-Cad and of its binding partners Arm and α -Cat appeared mostly normal in *Girdin* M/Z mutant embryos (Fig. 4A-M). This suggests that DE-Cad trafficking is not the primary mechanism through which Girdin regulates cell-cell adhesion. We also found that similar amounts of DE-Cad and α -Cat co-precipitated with Arm in wild-type and *Girdin* mutant embryos (Fig. 4N), suggesting that Girdin

has a limited, if any, impact on the assembly of this core adhesion complex. Robust cell-cell adhesion requires linkage of adherens junction components to the actin cytoskeleton (Harris and Tepass, 2010). Both fly and mammalian Girdin promote actin organization [this study; Enomoto et al. (2005); Puseenam et al. (2009)], and we found that Girdin is present in the cytoskeletal fraction together with DE-Cad and Arm, using biochemical fractionation of soluble and cytoskeleton-associated proteins (Fig. 4O) (Laprise et al., 2002). In addition, Girdin co-precipitated with α -Cat and actin (Fig. 4P). These data suggest that Girdin plays a role at the interface of the cadherin-catenin complex and the cytoskeleton. Accordingly, the association of DE-Cad, Arm and α -Cat with the cytoskeleton was decreased in the absence of Girdin (Fig. 4Q).

In conclusion, our study suggests that Girdin is required for epithelial tissue morphogenesis and integrity. Specifically, Girdin coordinates collective cell migration, a function that probably depends on the ability of Girdin to organize the actin cytoskeleton. Moreover, our data indicate that Girdin strengthens cell-cell adhesion by promoting anchorage of the cadherin-catenin complex to the cytoskeleton. Girdin might realize this function by favoring the polymerization and organization of the cortical F-actin ring associated with the ZA (Harris and Tepass, 2010; Puseenam et al., 2009). Alternatively, Girdin might be directly involved in the bridging of the cadherin-catenin complex to microfilaments, an intriguing possibility suggested by the association of Girdin with α -Cat. Multiple α -Cat interaction partners have actin-binding activity, and so do Girdin and mammalian Girdin (Enomoto et al., 2005; Harris and Tepass, 2010). Our data therefore contribute to the understanding of adherens junction regulation, which is crucial for epithelial tissue morphogenesis, physiology and homeostasis. It is likely that the function of Girdin in epithelial tissue cohesion and morphogenesis is evolutionarily conserved, as mammalian Girdin interacts with Par-3 that sustains cell-cell cohesion, and controls epithelial cyst formation in three-dimensional (3D) cell culture (Ohara et al., 2012; Ooshio et al., 2007; Xue et al., 2013). In line with a putative role for mammalian Girdin in cell-cell adhesion, neuroblasts show cohesion defects in Girdin knockout mice (Wang et al., 2011). Thus, our data put into perspective the emerging idea that human Girdin is an interesting target to limit cell invasion in cancer (Jiang et al., 2008; Weng et al., 2010). Girdin inhibition might exacerbate loss of cell-cell adhesion and cell dissemination in tumor cells with altered E-cadherin functions, as suggested by the strong enhancement of the *shg* zygotic mutant phenotype by loss of Girdin. A better understanding of Girdin functions will help to uncover whether this protein is an attractive target for therapeutic intervention.

MATERIALS AND METHODS

Molecular biology, DNA cloning and generation of transgenic lines

DNA fragments were PCR-amplified using the CloneAmp HiFi PCR Premix (Clontech) and subcloned in pUASTattB (kindly provided by K. Basler, University of Zurich, Switzerland), using the In-Fusion cloning kit (Clontech) according to the manufacturer's instructions. Positive clones were fully sequenced and injected in *Drosophila* embryos (BestGene). Transgenes were targeted using the PhiC31 integrase-mediated transgenesis system (Groth et al., 2004) in a fly line carrying an attP docking site (generated by K. Basler's group; Bloomington Stock number 24749). The following transgenic lines were generated: *UAS-Girdin* (expression of wild-type Girdin-PA; www.flybase.org) and *UAS-3XFlag-Girdin* (expression of Girdin-PA fused to a triple Flag tag at the N-terminus).

Drosophila genetics

Girdin¹ and *Girdin²* alleles were generated by imprecise P-element excision of P{SUPor-P} PGirdin[KG07727] (Bellen et al., 2004). *Girdin²* deleted

364 bp of the *Girdin* 5' UTR and 75 bp of the ORF, including the initiation codon. *Girdin¹* retained 996 bp of the 5' end of P{SUPor-P} Girdin [KG07727] within *Girdin* 5' UTR. *Girdin^{co6007}* results from the insertion of a PiggyBac transposon in the fourth exon of *Girdin* [Bloomington Stock number 14649; see Bellen et al. (2011); Thibault et al. (2004)]. *Girdin²* lethality was rescued by crossing *daGAL4*, *Girdin²* recombinant flies to *UAS-Girdin-PA*, *Girdin²* recombinant animals.

Girdin maternal and zygotic (M/Z) mutant embryos were obtained from *Girdin* germline clone females (P{ry[+7.2]=hsFLP}1, y[1] w[1118]; FRT9D P{ovoD1-18}3L/FRT9D, *Girdin*) that were heat-shocked twice for 2 h at 37°C as second- and third-instar larvae and crossed to *Girdin*/TM3, *act-GFP* males.

Antibody production

Polyclonal antibodies against Girdin amino acid 363-463 in fusion with GST were produced in guinea pigs. The antibody used in this study is referred to as anti-Girdin 163.

Immunofluorescence

Embryos were heat-fixed in E-wash buffer (7% NaCl, 0.5% Triton X-100) at 80°C, which was immediately cooled down by addition of ice-cold E-wash (Gamblin et al., 2014). Embryos were then rinsed with PBS and placed in methanol under a heptane phase, devitellinized by strong agitation and further incubated for 1 h in fresh methanol. Phalloidin and DE-cad staining were performed on embryos fixed in 10% paraformaldehyde for 30 min and devitellinized by hand. Following fixation, embryos were saturated in NGT (2% normal goat serum, 0.3% Triton X-100 in PBS) for 1 h at room temperature. Primary antibodies were diluted in NGT and incubated overnight at 4°C under agitation. Primary antibodies used were: guinea pig anti-Girdin 163 (this study, see above; 1:500); rat anti-Crb (Pellikka et al., 2002; 1:500); mouse anti-Crb [clone Cq4, Developmental Studies Hybridoma Bank (DHSB); 1:25]; mouse anti-Arm (clone N2 7A1, DHSB; 1:100); and rat anti-DE-Cad (clone DCAD2, DHSB; 1:50). Secondary antibodies were conjugated to Cy3 (Jackson ImmunoResearch Laboratories), Alexa Fluor 488 (Molecular Probes) or Alexa Fluor 647 (Jackson ImmunoResearch Laboratories), and used at a dilution of 1:500 in NGT (1 h, room temperature). Alexa Fluor 568-coupled phalloidin was used at a concentration of 0.5 U/ml and co-incubated with secondary antibodies. Embryos were mounted in Vectashield mounting medium (Vector Labs).

Cuticle preparation

Embryos were dechorionated, mounted in 100 μ l of Hoyer's mounting media (30 g of gum Arabic, 50 ml of distilled water, 200 g of chloral hydrate, 20 ml of glycerol)/lactic acid (1:1) and incubated overnight at 85°C.

Western blot

Dechorionated embryos were homogenized in one of the following buffers: (1) Triton lysis buffer [1% Triton X-100, 100 mM NaCl, 5 mM EDTA, 50 mM Tris (pH 7.6), 40 mM β -glycerophosphate, 50 mM NaF, 5% glycerol]; (2) RIPA buffer (1 \times PBS, 1% NP-40, 0.5% deoxycholate, 0.1% SDS, 1 mM sodium orthovanadate) or SDS buffer [15 mM Tris (pH 7.6), 5 mM EDTA, 2.5 mM EGTA, 1% SDS] supplemented with a protease and phosphatase inhibitor mix [1 mM phenylmethylsulfonyl fluoride (PMSF), 0.5 μ g/ml leupeptin, 0.7 μ g/ml pepstatin, 0.5 μ g/ml aprotinin and 0.1 mM orthovanadate]. Protein samples were then processed for SDS-PAGE and western blotting as described (Laprise et al., 2002). Primary antibodies used were: guinea pig anti-Girdin 163 (1:5000); mouse anti-Arm (clone N2 7A1, DHSB; 1:1000); rat anti-DE-Cad (clone DCAD2, DHSB; 1:100); rat anti- α -Cat (clone DCAT-1, DHSB; 1:1000); mouse anti-GAPDH (GAIR, Medimabs; 1:2000); mouse anti-actin (clone C4, Chemicon; 1:10,000), mouse anti-Flag (clone M2, Sigma; 1:2500). HRP-conjugated secondary antibodies were used at a 1:1000 dilution.

Immunoprecipitation

Embryos were homogenized in ice-cold Triton buffer (see 'Western blot' section), and debris was removed by centrifugation. 2 μ g of anti-Arm, anti-Flag or of purified mouse IgG (Invitrogen) were added to embryo lysate

(1.5 mg of total proteins) and incubated for 2 h at 4°C under agitation. Protein G-sepharose beads (GE Healthcare, 50% suspension in lysis buffer, 50 µl) were then added and further incubated for 1 h at 4°C under agitation. Immunocomplexes were harvested by centrifugation and washed five times with lysis buffer. Proteins were eluted with Laemmli buffer at 95°C for 5 min.

Isolation of cytoskeleton-associated proteins

Soluble proteins were extracted from dechorionated embryos using ice-cold lysis/cytoskeleton stabilization buffer [0.5% Triton X-100, 50 mM NaCl, 10 mM PIPES (pH 6.8), 300 mM sucrose, 3 mM MgCl₂] supplemented with the protease and phosphatase inhibitor mix (see 'Western blot' section). Samples were then centrifuged (17,000 g for 20 min at 4°C), and cytoskeleton-associated proteins (pellet) were solubilized in SDS buffer (see 'Western blot' section) at 95°C for 5 min.

Acknowledgements

We are grateful to K. Basler, the Bloomington Drosophila Stock Center and the Developmental Studies Hybridoma Bank for DNA constructs, fly stocks and antibodies, respectively. Confocal microscopy was performed at the CRCHU-Hôtel-Dieu imaging facility. DNA sequencing was carried out at the Genome Sequencing and Genotyping Platform of the CHU de Québec Research Center.

Competing interests

The authors declare no competing or financial interests.

Author contributions

P.L. and E.H. designed the project, performed the experiments and wrote the paper. P.L. initiated the project and generated some of the genetic and molecular tools used in this study while being in the laboratory of U.T., who also edited the manuscript.

Funding

This work was supported by operating grants from the Canadian Institute of Health Research (CIHR) to P.L. and U.T. [MOP-84249 and MOP-14372, respectively]. P.L. is a Fonds de Recherche du Québec-Santé (FRQ-S) junior 2 scholar. E.H. is a grantee from Harley Davidson Owners Group (chapitre de Québec)/fondation du CHU fund.

Supplementary material

Supplementary material available online at <http://dev.biologists.org/lookup/suppl/doi:10.1242/dev.122002/-/DC1>

References

- Asai, M., Asai, N., Murata, A., Yokota, H., Ohmori, K., Mii, S., Enomoto, A., Murakumo, Y. and Takahashi, M. (2012). Similar phenotypes of Girdin germ-line and conditional knockout mice indicate a crucial role for Girdin in the nestin lineage. *Biochem. Biophys. Res. Commun.* **426**, 533-538.
- Bellen, H. J., Levis, R. W., Liao, G., He, Y., Carlson, J. W., Tsang, G., Evans-Holm, M., Hiesinger, P. R., Schulze, K. L., Rubin, G. M. et al. (2004). The BDGP gene disruption project: single transposon insertions associated with 40% of Drosophila genes. *Genetics* **167**, 761-781.
- Bellen, H. J., Levis, R. W., He, Y., Carlson, J. W., Evans-Holm, M., Bae, E., Kim, J., Metaxakis, A., Savakis, C., Schulze, K. L. et al. (2011). The Drosophila gene disruption project: progress using transposons with distinctive site specificities. *Genetics* **188**, 731-743.
- Chou, T. B. and Perrimon, N. (1996). The autosomal FLP-DFS technique for generating germline mosaics in Drosophila melanogaster. *Genetics* **144**, 1673-1679.
- David, D. J., Tishkina, A. and Harris, T. J. (2010). The PAR complex regulates pulsed actomyosin contractions during amnioserosa apical constriction in Drosophila. *Development* **137**, 1645-1655.
- Desai, R., Sarpal, R., Ishiyama, N., Pellikka, M., Ikura, M. and Tepass, U. (2013). Monomeric alpha-catenin links cadherin to the actin cytoskeleton. *Nat. Cell Biol.* **15**, 261-273.
- Enomoto, A., Murakami, H., Asai, N., Morone, N., Watanabe, T., Kawai, K., Murakumo, Y., Usukura, J., Kaibuchi, K. and Takahashi, M. (2005). Akt/PKB regulates actin organization and cell motility via Girdin/APE. *Dev. Cell* **9**, 389-402.
- Enomoto, A., Ping, J. and Takahashi, M. (2006). Girdin, a novel actin-binding protein, and its family of proteins possess versatile functions in the Akt and Wnt signaling pathways. *Ann. N. Y. Acad. Sci.* **1086**, 169-184.
- Enomoto, A., Asai, N., Namba, T., Wang, Y., Kato, T., Tanaka, M., Tatsumi, H., Taya, S., Tsuboi, D., Kuroda, K. et al. (2009). Roles of disrupted-in-schizophrenia 1-interacting protein girdin in postnatal development of the dentate gyrus. *Neuron* **63**, 774-787.
- Franke, J. D., Montague, R. A. and Kiehart, D. P. (2005). Nonmuscle myosin II generates forces that transmit tension and drive contraction in multiple tissues during dorsal closure. *Curr. Biol.* **15**, 2208-2221.
- Friedl, P. and Gilmour, D. (2009). Collective cell migration in morphogenesis, regeneration and cancer. *Nat. Rev. Mol. Cell Biol.* **10**, 445-457.
- Gambin, C. L., Hardy, E. J.-L., Chartier, F. J.-M., Bisson, N. and Laprise, P. (2014). A bidirectional antagonism between aPKC and Yurt regulates epithelial cell polarity. *J. Cell Biol.* **204**, 487-495.
- Ghosh, P., Garcia-Marcos, M., Bornheimer, S. J. and Farquhar, M. G. (2008). Activation of Galphai3 triggers cell migration via regulation of GIV. *J. Cell Biol.* **182**, 381-393.
- Groth, A. C., Fish, M., Nusse, R. and Calos, M. P. (2004). Construction of transgenic Drosophila by using the site-specific integrase from phage phiC31. *Genetics* **166**, 1775-1782.
- Harden, N. (2002). Signaling pathways directing the movement and fusion of epithelial sheets: lessons from dorsal closure in Drosophila. *Differentiation* **70**, 181-203.
- Harris, T. J. C. and Peifer, M. (2004). Adherens junction-dependent and -independent steps in the establishment of epithelial cell polarity in Drosophila. *J. Cell Biol.* **167**, 135-147.
- Harris, T. J. C. and Tepass, U. (2010). Adherens junctions: from molecules to morphogenesis. *Nat. Rev. Mol. Cell Biol.* **11**, 502-514.
- Jiang, P., Enomoto, A., Jijiwa, M., Kato, T., Hasegawa, T., Ishida, M., Sato, T., Asai, N., Murakumo, Y. and Takahashi, M. (2008). An actin-binding protein Girdin regulates the motility of breast cancer cells. *Cancer Res.* **68**, 1310-1318.
- Kiehart, D. P., Galbraith, C. G., Edwards, K. A., Rickoll, W. L. and Montague, R. A. (2000). Multiple forces contribute to cell sheet morphogenesis for dorsal closure in Drosophila. *J. Cell Biol.* **149**, 471-490.
- Kitamura, T., Asai, N., Enomoto, A., Maeda, K., Kato, T., Ishida, M., Jiang, P., Watanabe, T., Usukura, J., Kondo, T. et al. (2008). Regulation of VEGF-mediated angiogenesis by the Akt/PKB substrate Girdin. *Nat. Cell Biol.* **10**, 329-337.
- Kowalczyk, A. P. and Nanes, B. A. (2012). Adherens junction turnover: regulating adhesion through cadherin endocytosis, degradation, and recycling. *Subcell. Biochem.* **60**, 197-222.
- Laprise, P., Chailier, P., Houde, M., Beaulieu, J.-F., Boucher, M.-J. and Rivard, N. (2002). Phosphatidylinositol 3-kinase controls human intestinal epithelial cell differentiation by promoting adherens junction assembly and p38 MAPK activation. *J. Biol. Chem.* **277**, 8226-8234.
- Matsushita, E., Asai, N., Enomoto, A., Kawamoto, Y., Kato, T., Mii, S., Maeda, K., Shibata, R., Hattori, S., Hagikura, M. et al. (2011). Protective role of Gipiie, a Girdin family protein, in endoplasmic reticulum stress responses in endothelial cells. *Mol. Biol. Cell* **22**, 736-747.
- McGill, M. A., McKinley, R. F. A. and Harris, T. J. C. (2009). Independent cadherin-catenin and Bazooka clusters interact to assemble adherens junctions. *J. Cell Biol.* **185**, 787-796.
- Morais-de-Sá, E., Mirouse, V. and St Johnston, D. (2010). aPKC phosphorylation of Bazooka defines the apical/lateral border in Drosophila epithelial cells. *Cell* **141**, 509-523.
- Muller, H. A. and Wieschaus, E. (1996). armadillo, bazooka, and stardust are critical for early stages in formation of the zonula adherens and maintenance of the polarized blastoderm epithelium in Drosophila. *J. Cell Biol.* **134**, 149-163.
- Ohara, K., Enomoto, A., Kato, T., Hashimoto, T., Isotani-Sakakibara, M., Asai, N., Ishida-Takagishi, M., Weng, L., Nakayama, M., Watanabe, T. et al. (2012). Involvement of Girdin in the determination of cell polarity during cell migration. *PLoS ONE* **7**, e36681.
- Ooshio, T., Fujita, N., Yamada, A., Sato, T., Kitagawa, Y., Okamoto, R., Nakata, S., Miki, A., Irie, K. and Takai, Y. (2007). Cooperative roles of Par-3 and aFadin in the formation of adherens and tight junctions. *J. Cell Sci.* **120**, 2352-2365.
- Pellikka, M., Tanentzapf, G., Pinto, M., Smith, C., McGlade, C. J., Ready, D. F. and Tepass, U. (2002). Crumbs, the Drosophila homologue of human CRB1/RP12, is essential for photoreceptor morphogenesis. *Nature* **416**, 143-149.
- Puseenam, A., Yoshioka, Y., Nagai, R., Hashimoto, R., Suyari, O., Itoh, M., Enomoto, A., Takahashi, M. and Yamaguchi, M. (2009). A novel Drosophila Girdin-like protein is involved in Akt pathway control of cell size. *Exp. Cell Res.* **315**, 3370-3380.
- Simpson, F., Martin, S., Evans, T. M., Kerr, M., James, D. E., Parton, R. G., Teasdale, R. D. and Wicking, C. (2005). A novel hook-related protein family and the characterization of hook-related protein 1. *Traffic* **6**, 442-458.
- Solon, J., Kaya-Copur, A., Colombelli, J. and Brunner, D. (2009). Pulsed forces timed by a ratchet-like mechanism drive directed tissue movement during dorsal closure. *Cell* **137**, 1331-1342.
- Tepass, U., Theres, C. and Knust, E. (1990). crumbs encodes an EGF-like protein expressed on apical membranes of Drosophila epithelial cells and required for organization of epithelia. *Cell* **61**, 787-799.
- Tepass, U., Gruszynski-DeFeo, E., Haag, T. A., Omatyar, L., Torok, T. and Hartenstein, V. (1996). shotgun encodes Drosophila E-cadherin and is preferentially required during cell rearrangement in the neurectoderm and other morphogenetically active epithelia. *Genes Dev.* **10**, 672-685.

- Thibault, S. T., Singer, M. A., Miyazaki, W. Y., Milash, B., Dompe, N. A., Singh, C. M., Buchholz, R., Demsky, M., Fawcett, R., Francis-Lang, H. L. et al.** (2004). A complementary transposon tool kit for *Drosophila melanogaster* using P and piggyBac. *Nat. Genet.* **36**, 283-287.
- Uemura, T., Oda, H., Kraut, R., Hayashi, S., Kotaoka, Y. and Takeichi, M.** (1996). Zygotic *Drosophila* E-cadherin expression is required for processes of dynamic epithelial cell rearrangement in the *Drosophila* embryo. *Genes Dev.* **11**, 659-671.
- Wang, Y., Kaneko, N., Asai, N., Enomoto, A., Isotani-Sakakibara, M., Kato, T., Asai, M., Murakumo, Y., Ota, H., Hikita, T. et al.** (2011). Girdin is an intrinsic regulator of neuroblast chain migration in the rostral migratory stream of the postnatal brain. *J. Neurosci.* **31**, 8109-8122.
- Weng, L., Enomoto, A., Ishida-Takagishi, M., Asai, N. and Takahashi, M.** (2010). Girding for migratory cues: roles of the Akt substrate Girdin in cancer progression and angiogenesis. *Cancer Sci.* **101**, 836-842.
- Weng, L., Enomoto, A., Miyoshi, H., Takahashi, K., Asai, N., Morone, N., Jiang, P., An, J., Kato, T., Kuroda, K. et al.** (2014). Regulation of cargo-selective endocytosis by dynamin 2 GTPase-activating protein girdin. *EMBO J.* **33**, 2098-2112.
- Xue, B., Krishnamurthy, K., Allred, D. C. and Muthuswamy, S. K.** (2013). Loss of Par3 promotes breast cancer metastasis by compromising cell-cell cohesion. *Nat. Cell Biol.* **15**, 189-200.
- Young, P. E., Richman, A. M., Ketchum, A. S. and Kiehart, D. P.** (1993). Morphogenesis in *Drosophila* requires nonmuscle myosin heavy chain function. *Genes Dev.* **7**, 29-41.

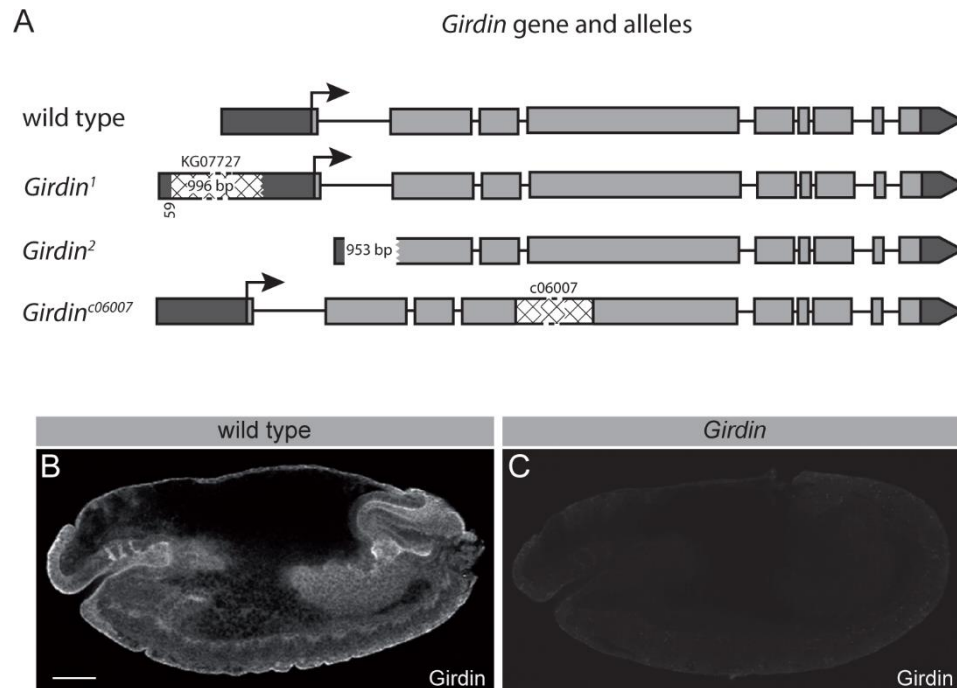


Figure S1. Genetic and molecular tools to study Girdin functions. A) Schematic representation of the *Girdin* gene, and of the mutant alleles used. The Girdin-PA isoform is encoded by an mRNA containing all exons of the *Girdin* gene. The allele *Girdin*² results from a 953 base pairs (bp) deletion removing 364 bp of the 5' UTR (dark grey), the start codon (arrow), the first intron and part of exon 2. The *Girdin*¹ allele retained 996 bp of the p-element KG07727 in the 5' UTR. *Girdin*^{c06007} results from the insertion of PBac PB Girdin[c06007] in the fourth exon of *Girdin*. B-C) Whole embryo view of a wild type embryo (B) or a *Girdin* M/Z mutant (C) immunostained with our Girdin antibody, which is potent and specific. Scale bar in B represents 50 μ m and also applies to C.